Soil Dynamics and Earthquake Engineering 31 (2011) 1607–1617

Contents lists available at ScienceDirect

Soil Dynamics and Earthquake Engineering

journal homepage: www.elsevier.com/locate/soildyn

A GIS-based earthquake damage assessment and settlement methodology

Mahdi Hashemi *, Ali Asghar Alesheikh

Department of Geospatial Information Systems, K.N. Toosi University of Technology, Mirdamad Cross, Valiasr Street, Tehran 19967-15433, Iran

ARTICLE INFO

Article history:
Received 16 January 2011
Received in revised form
21 June 2011
Accepted 5 July 2011
Available online 23 July 2011

ABSTRACT

Earthquakes have a greater effect on society than most people think. These effects range from structural damages to economic impacts and fatalities. An earthquake only lasts for a few seconds and the aftershocks may continue for days, but the damage does continue for years. Residential site safety and earthquake damage assessment studies play a crucial role in developing reliable rehabilitation and development programs, improving preparedness and mitigating losses in urbanized areas. The extremely densely populated metropolis of Tehran, which totals of 7,768,561 for 22 districts (according to the 2006 population census), coupled with the fragility of houses and infrastructure, highlight the necessity of a reliable earthquake damage assessment based on essential datasets, such as building resistance attributes, building population, soil structures, streets network and hazardous facilities. This paper presents a GIS-based model for earthquake loss estimation for a district in Tehran, Iran. Damages to buildings were calculated only for the ground shaking effect of one of the region's most active faults, the Mosha Fault in a likely earthquake scenario. Earthquake intensity for each building location was estimated based on attenuation relation and the ratio of damage was obtained from customized fragility curves. Human casualties and street blockages caused by collapsed buildings were taken into account in this study, as well. Finally, accessibility verification found locations without clear passages for temporary settlements by buildings via open streets. The model was validated using the 2003 Bam earthquake damages. The proposed model enables the decision-makers to make more reliable decisions based on various spatial datasets before and after an earthquake occurs. The results of the earthquake application showed total losses as follows: structural damages reaching 64% of the building stock, a death rate of 33% of all the residents, a severe injury rate reaching 27% of the population and street closures upwards of 22% due to building collapse.

1. Introduction

Metropolises are specifically vulnerable to earthquakes due to the high density of buildings, infrastructure and people [1]. Highly populated cities that are unprepared for such emergencies contain many potential victims and invite high fatalities during unavoidable disasters [2–4]. Although rare in Tehran metropolis, earthquakes are one of the most destructive natural hazards, so assessing the damage they cause is of great importance [5]. Disaster management and mitigation are not easy tasks and require resources and analyses to design effective and appropriate strategies to reduce vulnerability [6,7]. This complexity dictates the use of an integrated earthquake damage assessment methodology. The design of geographic information systems (GIS) supports spatial decision-making based on multiple georeferenced datasets and it thereby makes possible natural disaster risk assessment for vulnerability reduction [8–10]. For the purpose of this paper, the GIS data layers of the study area include the dwelling unit inventory, statistical information about buildings, streets, the positions of hazardous facilities (e.g., gas stations), active faults and soil characteristics. The collected data were corrected and converted to shape files and geodatabases. The information such as distances of buildings to the Mosha Fault and street widths were extracted from primary layers. We used ArcGIS toolbox functions to analyze the data layers and present final damages. This study highlighted the usefulness of GIS for the input, management, manipulation, analysis and visualization of spatially referenced data.

Although residential regions are at risk because of multiple hazards caused by earthquakes, including landslides, surface fault rupture, tsunami, liquefication, fire and flood as well as the release of hazardous materials, ground shaking is the principal cause of earthquake damage and loss [13,15,8]. The primary objective of this study is to develop earthquake loss scenarios in terms of building and street damages and casualties. Damage to buildings was calculated only from the ground shaking effect of an earthquake.

* Corresponding author. Tel.: +98 21 8878 6212; fax: +98 21 8878 6213.
E-mail addresses: m.hashemi1987@gmail.com (M. Hashemi), alesheikh@kntu.ac.ir (A.A. Alesheikh).

0267-7261/$ - see front matter © 2011 Elsevier Ltd. All rights reserved.
doi:10.1016/j.soildyn.2011.07.003

For the calculation of ground shaking effects on buildings, Modified Mercalli Intensity (*MMI*) attenuation relation was modified for local geology. The building's damages were estimated based on the fragility curves. Casualties were estimated for each building based on its damage, structure and occupancy at the time of the incident. An approach for determining the percent of streets blocked was developed and buildings without clear access to temporary settlements were identified.

This paper is organized into 7 sections. Section 1 presents the importance of the subject and evaluates some important attempts related to the purpose of this paper. In Section 2, the proposed methodology will be discussed in detail. The application for a parish in Tehran as well as the results will be presented in Sections 3 and 4, respectively. Validation of the model on 2003 Bam earthquake is discussed in Section 5. Sensitivity analysis of model parameters is presented in Section 6. Finally, the conclusion will be stated in Section 7.

1.1. Background

There are several disaster management and damage assessment methodologies practiced around the world [11]. Michalowski et al. [12] presented a decision support system for disaster management that was established by NEGOPLAN, an expert system shell for negotiation support. This framework was developed to test the accuracy of a disaster manager's decisions. Bird and Bommer [13] considered ground failure and shaking as causes of damage in their analysis of survey data and presented their relative contribution to general damage in each section of the regional infrastructure. Ergonul [14] studied the economic aspects of earthquakes and presented a probabilistic model for loss assessment in a town at risk for earthquakes. His model simulated the potential benefits of various pre- and post-earthquake mitigation strategies within the framework of Monte Carlo. His model measured the severity of the earthquake, building resistance and soil structure, which determined the value of the recovery cost. Montoya and Masser [1] demonstrated how a risk evaluation is performed using GIS to produce the cost-benefit scenarios that in turn enhance the transparency of the decision-making process. They first developed a list of datasets required to extract a risk assessment, an approach to integrate these datasets and a method to assess costs and benefits of mitigation measures. Karimi and Hüllermeier [5] presented a fuzzy system for evaluating the risk of natural hazards under highly uncertain conditions. Uncertainties regarding the probability of occurrence and disaster severity in a region have been represented in terms of fuzzy probability. Uncertainties concerning the correlation between the parameters of the natural disaster and its consequent damages and losses have been considered by means of fuzzy relations. Moreover, the combination of fuzzy probability of hazard and fuzzy vulnerability relation produced the fuzzy probability of damage. Feyza Cinicioglu et al. [15] evaluated the risk from each damage-causing effect including ground shaking, liquefaction, landslide and seismic bearing capacity degradation separately at a rationally rigorous level and then integrated the risks. This approach is related to soil structure interactions by quantifying site-specific structural and geotechnical properties. We use Feyza Cinicioglu's attenuation relation to accomplish a part of our objectives. Srinivas and Nakagawa [16] emphasized the cyclical linkages between environmental reduction and its exacerbation of a hazard's effects and environmental impacts by verifying the evaluations of the Indian Ocean earthquake and tsunami that struck on 26 December, 2004. They also discussed the use of environmental management for disaster mitigation but our work discusses the urban management. Tinguaro Rodriguez et al. [17] presented a new version of Systems Experted for Disaster Diagnosis (SEDD), which uses fuzzy logic. The SEDD methodology is an inductive data-based approach which scans and analyzes a large database of historical disasters to produce fuzzy rules, which can be used to evaluate the consequences of almost any possible disaster scenario. The main objective of SEDD is to support Non-Governmental Organization (NGO) decision-makers involved in international response, who bring relief to people affected by a natural disaster. Ansal et al. [18] integrated deterministic hazard scenarios and time-dependent probabilistic hazard assessment into a GIS-based loss assessment model of Istanbul, Turkey, to develop loss scenarios in terms of structural damage and fatalities. We profit from their method for the estimation of casualties.

2. Material and methods

2.1. Study area

The metropolis of Tehran, located at the southern foothills of the Alpine–Himalayan orogen in Iran, has an area of about 614 km^2 and is divided into 22 districts [19–21]. Seismologists believe that an intense earthquake may strike Tehran in the near future because the city has not experienced a powerful earthquake since 1830 [22–24]. The Mosha Fault is situated about 30 km above Tehran (Fig. 1) and seems to be among the most active faults in this region, experiencing major earthquakes with magnitudes more than 6.5 in the years 958, 1665 and 1830 [25,19]. Hamzehloo et al. [27] estimated that the maximum credible earthquake for faults around Tehran varies in the range of 6.2–7.3 by considering the length of the faults. Zafarani et al. [26] indicated that the Mosha Fault, over 200 km long, can cause earthquakes up to a magnitude of 7.4 with focal depths ranging from 13 to 30 km. Thus, the predicted magnitude for the Mosha fault future earthquake is almost between 6.4 and 7.4 based on the mentioned works and historical earthquakes. In our research, two scenarios with magnitudes of 7.4 and 6.4 were considered for this fault.

The developed methodology was applied to the south Karoon parish in Region 10 of Tehran, Iran. Fig. 1 shows the location of study area with respect to the Mosha Fault. The study area is bounded between longitudes of 51°21′50″–51°22′12″ E and latitudes of 35°40′50″–35°41′24″N. There are 71 blocks, 3737 parcels, 5293 buildings and 26,498 people in the southern Karoon parish. All buildings have less than 7 stories and several old structures vulnerable to a major earthquake exist. The building stock consists of 21% steel, 5% reinforced concrete, 11% steel and brick and 63% adobe.

2.2. Data preparation

Needed information were obtained from Prevention and Crisis Management Organization and International Institute of Earthquake Engineering and Seismology (IIEES) in Tehran.

In this study, the dwelling unit inventory database was prepared based on 2006 census data. Statistical information about buildings include their type of structure, number of stories and year of construction. The GIS data layer of parish streets was also obtained, verified and corrected by ground-based and official reviews. Next, data such as distances of buildings to the Mosha Fault and street widths, were extracted using ArcGIS software. Hazardous facilities, including gas stations, gas lines and major gas valves were identified as shape files for the location and analysis of temporary settlements and these sites included schools, mosques and earthquake-resistant open spaces [14]. All layers were converted to shape files and integrated in a geodatabase.

In the study area, there are no parks, nearby gas stations or high voltage transmission lines. There are, however, many gas

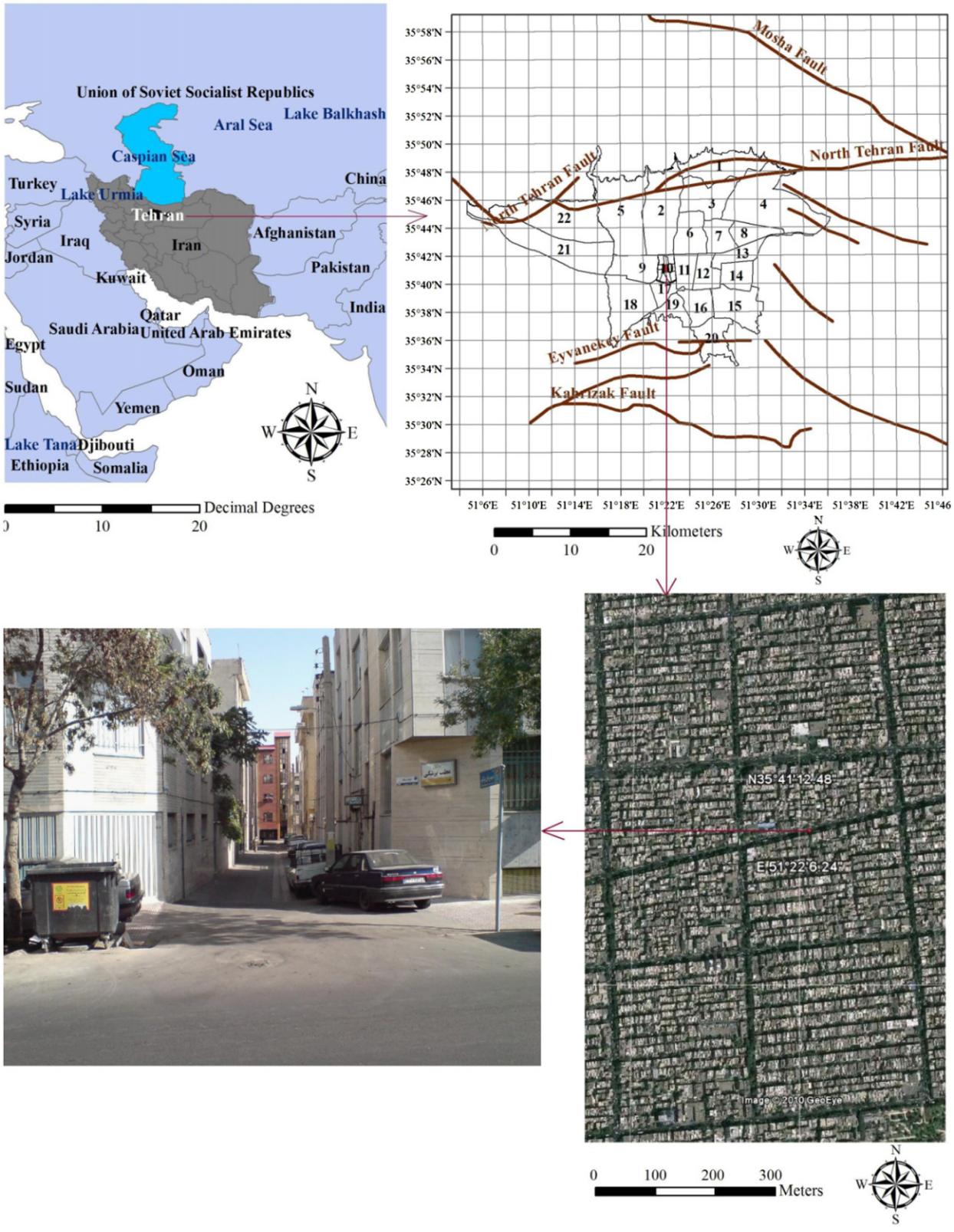

Fig. 1. Study area (top left) and a photograph from the south Karoon district showing its narrow streets (bottom left).

lines and major gas valves that pose a threat due to their manual valve shut-off manipulation systems. Shelters will be settled in schools, mosques and vacant parcels that are far enough from major gas valves to prevent destruction under modeled earthquakes.

2.3. Methodology

Earthquake loss assessments are predictions of possible damages and losses from future earthquakes. Risk estimation studies carried out in earthquake-prone areas over the world

indicate great diversity in terms of the sophistication of applications and the parameters included [28,8,10], but database preparation and the choice of the damage assessment method affect each other.

Our studies showed that there is not yet a standardized method for spatial damage estimation analysis. This paper develops a novel damage assessment methodology and applies it to a parish of Tehran, Iran. The main steps of the presented methodology can be followed through the flow chart given in Fig. 2. Ground shaking is considered as the main damage-causing phenomenon. For the calculation of the ground shaking effect on buildings, Modified Mercalli Intensity (*MMI*) attenuation relation was modified for local geology. The building's damages were estimated based on fragility curves that were developed for different building categories from the view point of resistance against ground shaking in Tehran [28]. Casualties were calculated for each building based on its damage and structure. After estimating the building waste materials, an approach for determining the percent of streets blocked was developed and buildings without clear access to temporary settlements were identified.

2.3.1. Intensity of earthquake on each structure

Ground shaking, the most devastating seismic hazard, is determined through a qualitative measure of its seismic intensity, or the severity of seismic ground motion at a specific location, a measurement used widely in engineering and seismology. In this study, the intensity-based characterization *MMI* is used because intensity characterization includes the impacts of local geology, the earthquake source characteristics, distance of the fault to the site, amplitude, duration, periodicity and frequency content of the earthquake [29]. Additionally, fragility curves based on *MMI* for different kinds of buildings in Tehran were also available. Many attempts have been made to relate seismic intensity to ground shaking parameters e.g., [30–36]. Within the context of this paper, *MMI* values for a specific site are calculated based on an earthquake scenario, earthquake source characteristics and site-specific geological and geotechnical data. The *MMI* of the ground motion for a specific site is first calculated by Eq. (1) as suggested by Crespellani et al. [37] and Feyza Cinicioglu et al. [15]. *MMI* increases (δI_{MMI}) due to local geology were obtained from Eq. (2), as given by Borcherdt [38] and Feyza Cinicioglu et al. [15]. Then, MMI^* was calculated based on Eq. (3) and expected to be common in the inspected area.

$$MMI = 8.6 + 1.48M - 6.4\log(d+14) \quad (1)$$

$$\delta I_{MMI} = 3.48\log(F_v) \quad (2)$$

$$MMI^* = MMI + \delta I_{MMI} \quad (3)$$

In the above equations, M stands for the magnitude of the earthquake, d is the distance from the desired location to the fault and F_v represents the amplification in the velocity band. Site amplification factors (F_a and F_v for short and longer periods, respectively) represent the amplification capability of the local soils with regards to uniform ground condition. These factors are based on the five site categories defined in terms of a representative average shear-wave velocity over a depth of 30 m [15]. Shafiee and Azadi [39] presented shear-wave velocity (v_s) characteristics for the different geological units throughout Tehran. They extended the existing results to other areas with the same material properties based on geological units. Finally, they used average shear-wave velocity to 30 m ($v_s(30)$) to produce a map of site conditions in Tehran by classification of geologic units with similar physical properties to the National Earthquake Hazard Reduction Program (NEHRP) categories. Their results are used in this study for finding F_v based on site factors established by new Standard AS/NZS 1170.4 [40] shown in Table 1.

2.3.2. Estimation of damage to buildings based on fragility curves

The resistance of buildings to earthquakes varies from area to area and from country to country. The relationship between seismic impact and the damage ratio differs, even if structures are similar to each other in appearance. It is considered that various construction approaches cause these differences. Gathering seismic hazards records and developing a damage function based on local experiences are the most important parts of damage assessment.

Askan and Yucemen [42] presented three probabilistic methods for the evaluation of potential seismic damage to low and mid-rise reinforced concrete (RC) buildings in Turkey. Rossetto and Elnashai [43] presented a new empirical fragility curves for European-type RC building populations based on a database of 99 post-earthquake damage distributions observed in 19 earthquakes

Table 1
Site Factors that show F_v and F_a for five different NEHRP categories, stipulated by new Standard AS/NZS 1170.4 [41].

Site class	A	B	C	D	E
F_a	0.80	1.00	1.25	1.25	1.25
F_v	0.80	1.00	1.40	2.25	3.50

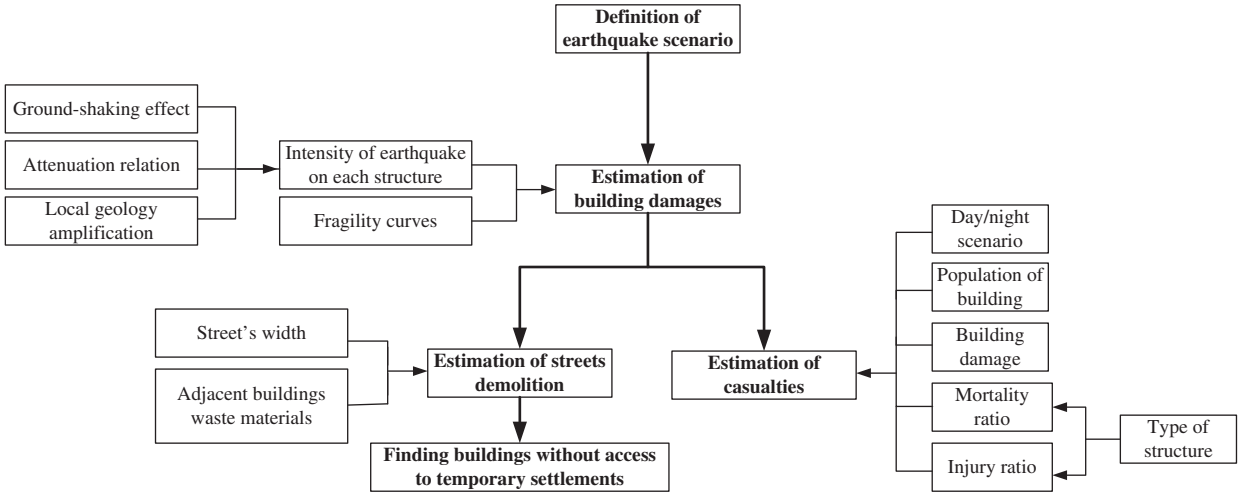

Fig. 2. Flow chart for the proposed methodology: main stages along with the used information to estimate the damages.

and regarding a total of 340,000 RC buildings. Some generic fragility curves were developed by Coburn and Spence [44] and fragility curves based on Iranian buildings were developed by JICA [28] and derived from damage observations to different structures in historical Iranian earthquakes (Fig. 3). Their study used building information like structural type, construction year and the number of stories. Based on this information, the buildings in the study area were categorized into 9 types, specifically noting building resistance (Table 2). The following fragility curves were used in this study for estimation of ground shaking-induced damage to buildings.

2.3.3. Estimation of casualties

Fatality estimation is notoriously difficult. Casualty numbers vary from one earthquake to the next and data documenting mortality rates is poor. The statistics recording casualties due to earthquakes present a wide range of causes of death including tsunamis, fires following earthquakes, rockfalls, landslides and other hazards. In most large-scale earthquake disasters, the main cause of fatalities is building collapse [18,22,44]. We believe that the casualty estimation is related to building damage estimation because the casualty number is principally due to the rate of people trapped in collapsed or heavily damaged buildings. During the 20th century, about 75% of the deaths attributed to earthquakes have been caused by the collapse of buildings [44].

Building collapse will also be the most notable cause of human casualty in Tehran because tsunamis do not affect the site and potential landslide sites are distributed only in the northern edge of the city [28]. Thus, only the human casualties caused by building collapse were taken into account in this study.

There are many similar attempts for calculation of casualties around the world e.g., [18,44,28], but this study calculates casualties for each building separately based on occupancy at the time of the incident, the building population, its damage percent and its lethality ratios in the following manner:

$$\text{Mortality} = \text{Occupancy ratio} \times \text{Population} \times \text{Damage percent} \times \text{Mortality ratio} \quad (4)$$

$$\text{Injured} = \text{Occupancy ratio} \times \text{Population} \times \text{Damage percent} \times \text{Injury ratio} \quad (5)$$

The "occupancy ratio" is assumed as 1 to estimate the number of casualties during night-time, when the residents are in their homes. The death ratio for daytime to night-time was correlated with the seismic intensity (*MMI*). In this correlation, previous actual damages in Iran were taken into account. The data for six earthquakes is shown in Table 3. Two earthquakes occurred during the day, when workers and students were absent from their homes. The other four earthquakes occurred in the early morning or during the night, when almost all residents were in their homes.

There is a distinct difference in death ratio in case of daytime and night-time earthquakes. It is considered that many people were outside their residential buildings and/or many people were in office buildings with stronger anti-seismic structures during the daytime.

Fig. 4 shows the relationship between seismic intensity (*MMI*) and the death ratio in daytime to night-time. This diagram is obtained from the interpolation of data in Table 3. Thus, the occupancy ratio in Eqs. (4) and (5) is obtained from this diagram, based on the seismic intensity (*MMI*).

For example, the occupancy ratio in the daytime is about 0.92 of that of the night-time for *MMI* 6.4. These results were derived from previous damage experiences and the effects of movements of the population and other variables were not considered.

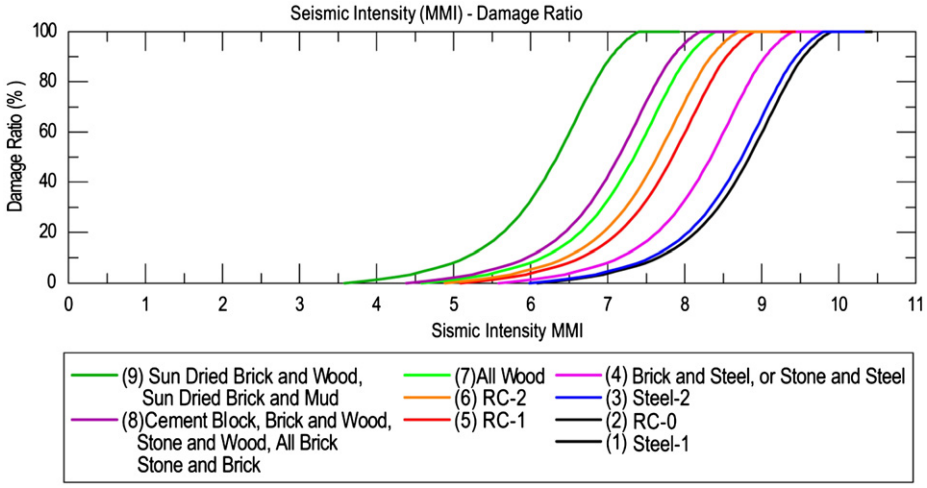

Fig. 3. Fragility curves indicating damage ratio based on *MMI* for different structural types in Tehran developed by JICA [28].

Table 2
Description of different structural types featuring building structural resistance.

1	Steel-1	Steel MRF structure, built after 1992, with 1 to 3 stories
2	RC-0	RC MRF structure, with more than 6 stories
3	Steel-2	Steel MRF structure, built before 1991 or with more than 4 stories
4	Brick and Steel, or Stone and Steel	
5	RC-1	RC MRF structure, built after 1991 and with 1 or 2 stories
6	RC-2	RC MRF structure, built before 1991 or with more than 3 stories
7	All Wood	
8	Cement Block, Brick and Wood, Stone and Wood, All Brick, Stone and Brick	
9	Sun Dried Brick and Wood, Sun Dried Brick and Mud	

Table 3
Death ratios for major historical Iranian earthquakes [28].

Earthquake	**Ghir**		**Tabas**		**Golbaft**		**Sirch**		**Manjil**		**Ardekul**	
Year	1972		1978		1981		1981		1990		1997	
Daytime/Night-time	Night-time		Night-time		Daytime		Night-time		Night-time		Daytime	
	MMI	Death	*MMI*	Death	*MMI*	Death	*MMI*	Death	*MMI*	Death	*MMI*	Death
Data for each village	9	67.1	10	84.3	7	9.2	9	57.1	6	0.79	10	2.7
	9	20.4	9	42.8			9	32.1	6	0.1	10	13.4
			9	19.2			8	9.8	6	0.0	9	23.1
			8	8.7			8	2.1	9	90.0	10	45.5
									10	90.0	8	6.5
									7	9.0	8	11.0
									10	66.7	8	1.7
									8	13.3	7	5.8
											8	3.0

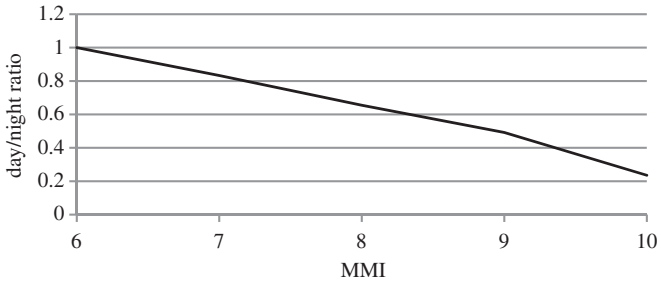

Fig. 4. Daytime/night-time fatality ratio obtained from historical Iranian earthquakes.

Table 4
Mortality and injury ratios for different building types in Tehran, Iran.

Building type	Mortality ratio	Injury ratio
RC buildings with 4 stories or more	1	0
RC buildings with less than 4 stories	0.8	0.2
Masonry buildings with 4 stories or more	0.6	0.4
Masonry buildings with less than 4 stories	0.5	0.5
Steel buildings with 4 stories or more	0.5	0.4
Steel buildings with less than 4 stories	0.4	0.4
Timber frame buildings	0.3	0.4

Each building class has its own specific set of lethality ratios that are developed based on native experts experiences and Coburn and Spence [44] (Table 4).

The casualties estimated in our proposed method will constitute most, but not all, of the expected fatalities. In addition to the casualties caused by structural failure, other probable causes of casualties should be taken into account including major secondary catastrophes mentioned above, the collapse of large civil engineering structures, the direct effects of fault rupture and miscellaneous other causes not considered here.

2.3.4. Estimation of street demolition

Streets in an earthquake zone have a crucial role in relief operations and traffic management; therefore, verification of their vulnerability during a disaster event is very important. Open spaces like streets are more resistant to earthquakes [14,11], but most routes are occupied by building waste materials after a heavy earthquake, especially in narrow streets adjacent to damaged tall buildings. In this study, the following method was applied to determine obstruction of streets adjacent to damaged buildings.

Eq. (6) calculates building volume and Eq. (7) calculates the volume of construction materials for each building developed by native civil engineers. The volume of building waste materials is calculated from Eq. (8) based on damage percent obtained in Section 2.3.2. A height of 1 m was considered for waste materials and the area occupied by them was calculated using Eq. (9). Finally, the area of streets occupied by waste from each adjacent building was calculated using Eq. (10).

$$\text{Volume of building} = \text{Area of ground floor} \times \text{Number of stories} \times \text{Height of each floor} \quad (6)$$

$$\text{Volume of construction materials} = \text{Volume of building}/5 \quad (7)$$

$$\text{Volume of waste materials} = \text{Volume of construction materials} \times \text{Percent of building damage} \quad (8)$$

$$\text{Area of waste materials} = \frac{\text{Volume of waste materials}}{\text{Height of waste materials}} \quad (9)$$

$$\text{Occupied area of adjacent street} = \text{Area of waste materials} - \text{Area of ground floor} \quad (10)$$

For buildings with two or three adjacent streets, obtained area from Eq. (10) was divided equally between them.

Streets were divided into small pieces (about 30 m) and the area of each segment was calculated. The buildings adjacent to each street segment were identified and their total potential construction waste was calculated and used in Eq. (11) to determine the occupied percent of each street segment.

$$\text{Occupied percent of each street segment} = \frac{\text{Occupied area}}{\text{Area of street segment} \times 100} \quad (11)$$

If the result of Eq. (11) is greater than 100, it indicates street blockage.

3. Case study

The probable magnitude of 7.4 for the Mosha Fault resulted in intensities (*MMI**) greater than 9.4. Verification of fragility curves in Fig. 3 indicates that such intensities could completely destroy all the buildings and therefore, a magnitude of 6.4 was adopted for the night-time scenario.

The epicentral distances of buildings in the study area were between 31,190 and 32,270 m. *MMI* intensities were found using the attenuation relationship presented in Eq. (1). The *MMI** was found using Eq. (3). Based on Table 1, F_v was determined as 1.4 for the study area because the area was categorized in class

C of NEHRP provisions by Shafiee and Azadi [39]. The results for *MMI** were between 7.92 and 7.99 for different epicentral distances.

Damage to buildings was calculated based on *MMI** obtained from previous steps and fragility curves shown in Fig. 3. Mortalities and injuries for each building and percent of streets occupied by waste materials were calculated based on the proposed methods (Sections 2.3.3 and 2.3.4). To estimate the fatalities, a night-time earthquake scenario was considered, so the occupancy ratio in Eqs. (4) and (5) was considered as 1.

4. Results of application

4.1. Damages to buildings, people and streets

GIS analysis of the results revealed that a magnitude of 6.4 will damage a range of 12–100% of all buildings, with 32% of buildings experiencing 12–33% total damage, 5% experiencing 64–72% damage and the remainder experiencing more than 91% damage. Fig. 5 presents expected damage levels for structures; red buildings are severely damaged and would require exercising special

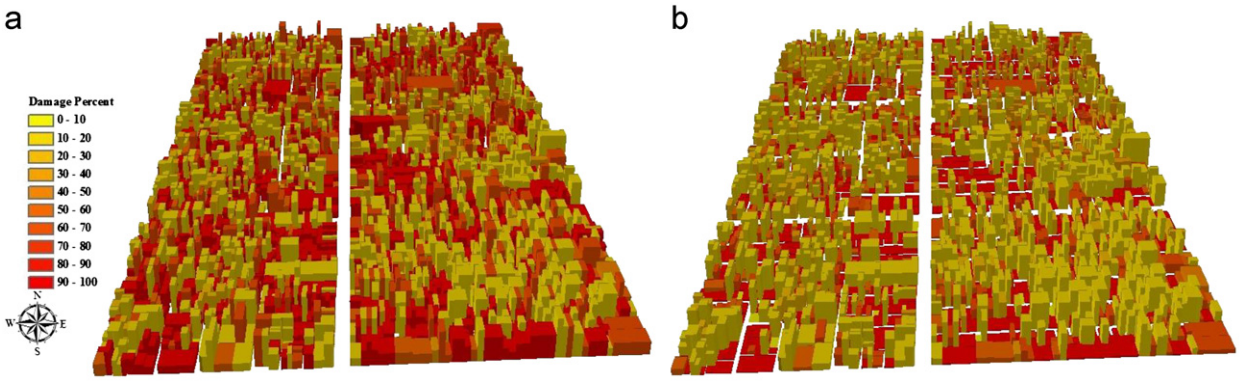

Fig. 5. (a) Primary heights of buildings: expected damage levels are indicated by the color bar. (b) Heights of buildings after modeled earthquake. (For interpretation of the references to color in this figure, the reader is referred to the web version of this article.)

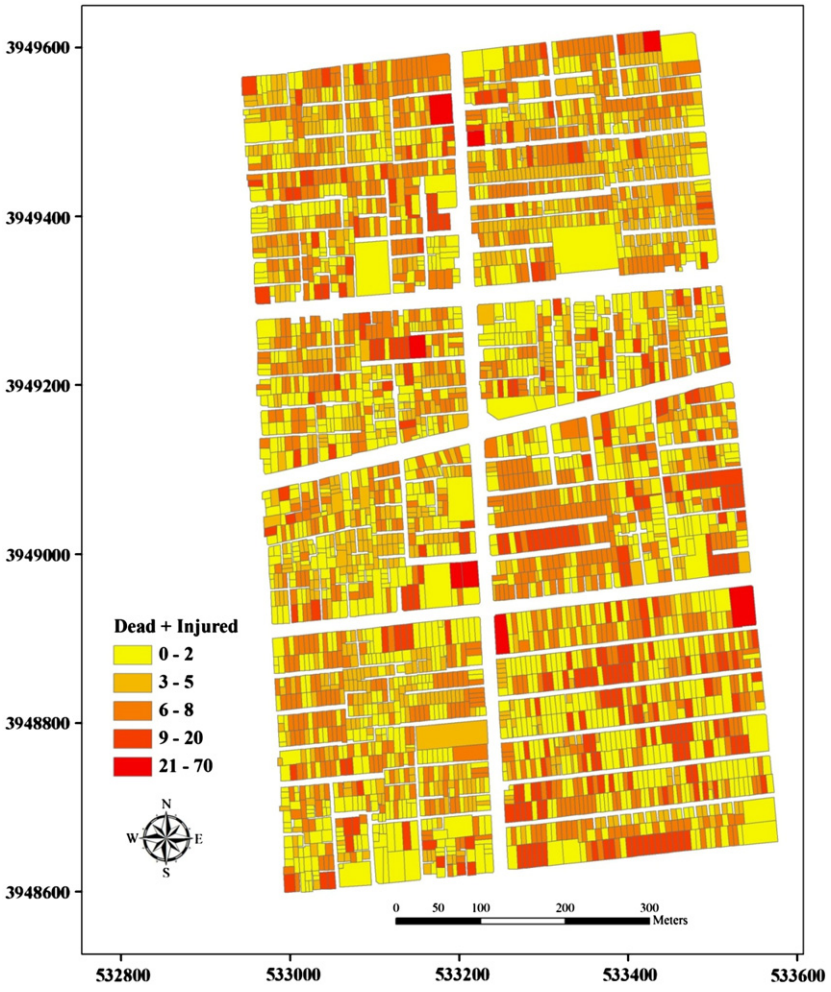

Fig. 6. The number of dead and injured people in each building.

precautions. In this figure, the heights of buildings before (Fig. 5a) and after (Fig. 5b) the modeled earthquake were calculated from Eqs. (12) and (13), respectively, using a 3 m floor height.

$$\text{Primary height} = \text{Number of stories} \times 3 \quad (12)$$

$$\text{Secondary height} = (1 - \text{Damage percent}) \times \text{Primary height} \quad (13)$$

Results of casualties estimation showed that about 8655 people out of 26,498 would be killed and about 7279 would suffer injuries. All people killed and injured in each building are shown in Fig. 6.

The only clinic situated in the parish, was damaged 16% and the only fire station was totally destroyed. According to these statistics, the region's crisis was severe.

Street damage caused by building waste materials is shown in Fig. 7. The occupied percent of border streets in the study area were doubled to account for the effects of buildings on each streetside. The total length of streets in the area is 22,244 m. After the modeled earthquake, 12% of streets were completely free, 48% were 1–50% blocked, 18% were by 51–100% blocked and 22% showed greater than 100% blockage by building waste materials. Streets with greater than 100% blockage are considered closed as shown in Fig. 7. Except for a few segments, major streets in the study area remained open because of their size, but many minor routes are closed. Fig. 1 represents a photograph taken from the district that displays blockages after the modeled earthquake.

4.2. Finding buildings without access to temporary settlements

Damage to all schools and mosques in the area is more than 50% and the only mosque with damage 18% is situated near major gas valves prohibiting it from becoming a safe temporary settlement. Seven vacant parcels in the area were considered as temporary settlements (Fig. 7). Their total area is 906 m^2. But that area does not likely provide enough space for earthquake victims. Finally, settlement accessibility was verified and buildings without clear passage to settlements were identified and marked red in Fig. 7. Almost all buildings in the southeastern part have no access to settlements, as shown in Fig. 7 and this results from the full breakdown streets in this area due to a high volume of waste and narrow streets.

The developed model in this paper can approximately predict the damage to buildings and streets. These measures can help disaster-managers in two ways; first, to mitigate damages. In our model, we classified buildings based on their vulnerability against the most probable future earthquake, so buildings should be reinforced or reconstructed based on their weaknesses. Some rules could be set up to limit structures' type to prohibit future damages. Also, many blocked streets (extracted from this model) can be widened in long-term strategies. Second application of this model is preparing paramedics to deal with the incident that is our future work. We have an estimation of damages and fatalities as well as the streets blockages due to the designed earthquake. Thus, we can consider all these issues for planning relief operations

Fig. 7. Street blockages by adjacent building waste materials (black lines); temporary settlements (blue points); buildings without access to settlements (red buildings). (For interpretation of the references to color in this figure legend, the reader is referred to the web version of this article.)

after the earthquake, locating and distributing paramedics, and determining relief paths in advance.

5. Validation of the model on Bam earthquake

On December 26, 2003 a large earthquake of M_w=6.5 shook the Bam district located in southeastern Iran [45]. Several dozen villages were destroyed and tens of them were severely damaged. More than 45,000 people were killed, and 30,000 were injured. The event was associated with a 9 km surface rupture of the Bam Fault. Houses in Bam were usually one-story masonry buildings and some of them were old and very weak [46,47]. Therefore, all buildings of this type totally collapsed during the earthquake. The earthquake intensity at the epicenter is determined as IX^+ (between 9 and 10) on the MSK scale, which strongly decreases with distance from the surface ruptures [46]. Although, a regular database, such as the one for Tehran, is not available for this city, and some of the site factors are a little different from those for Tehran, a part of the Bam City was adopted as a validating case for our model, because the building types are very similar and the damages are available. The validation location is depicted in Fig. 8. The distance between the study area and the earthquake source is about 3.5 km.

The soil classification used by Ahmadizadeh and Shakib [47] is the same as that of Iranian building code [48], where the average shear-wave velocity in soil layers falling in the upper 30 m of the site is the basis for soil classification. They classified the Bam station soil as type D in Table 1 by comparing the average shear-wave velocities in the Site Categorization Procedure of UBC-97 with those of Iran Standard No. 2008. Thus, an F_v=2.25 was assigned to the site.

The *MMI** was calculated as 11.49 for the study area, from Eq. (3). This result proves that the equation is rather pessimistic, because Bam earthquake intensity was estimated as 10 at worst [46]. We need to develop fragility curves for the buildings of the Bam City like the one for Tehran in Fig. 3 to estimate the damage percent to each building; although such intensity will totally destroy the one-story masonry buildings. This type includes more than 80% of the buildings of the city.

The above results showed that the model is almost pessimistic, but it is not a foible, rather a precaution. The perfect application of the GIS-based model for the City of Bam needs the perfect geodatabase of the city like the one for Tehran.

6. Sensitivity analysis of model parameters

The *MMI** was calculated from Eq. (3). The effects of the parameters' small changes on the final output are studied in this section. This equation is very sensitive to earthquake magnitude (M). With every 0.1 increase in earthquake magnitude, 1.4 is added to earthquake intensity. The amplification in the velocity band (F_v) has an effective role in changing *MMI**, after the magnitude. The derivative of *MMI** to F_v is shown in Fig. 9.

As the above diagram shows, in regions with a small F_v, the sensitivity of the *MMI** to the F_v increases. The sensitivity of the *MMI** in the study area (F_v=1.4) is calculated from Eq. 14 for small changes in F_v (i.e. an error of 0.1 in F_v results in an error of 0.1 in *MMI**).

$$\partial MMI^* = 1.08 \times \partial F_v \tag{14}$$

The distance from the earthquake source (d) is the third effective parameter on the earthquake intensity. The derivative of *MMI** to d is shown in Fig. 10. This diagram shows that the *MMI** is more sensitive to d in the closer regions to the earthquake source, but in the negative direction.

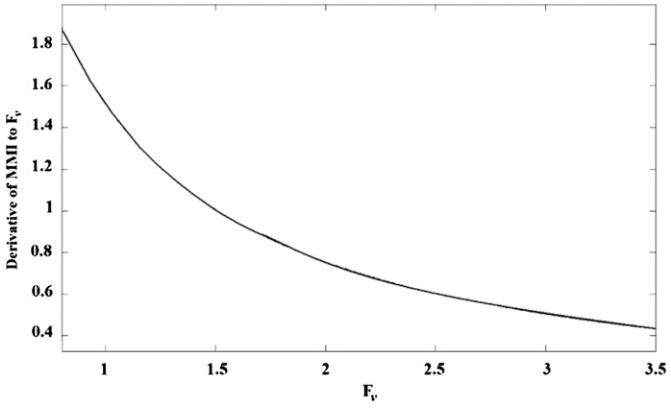

Fig. 9. The derivative of *MMI** to F_v.

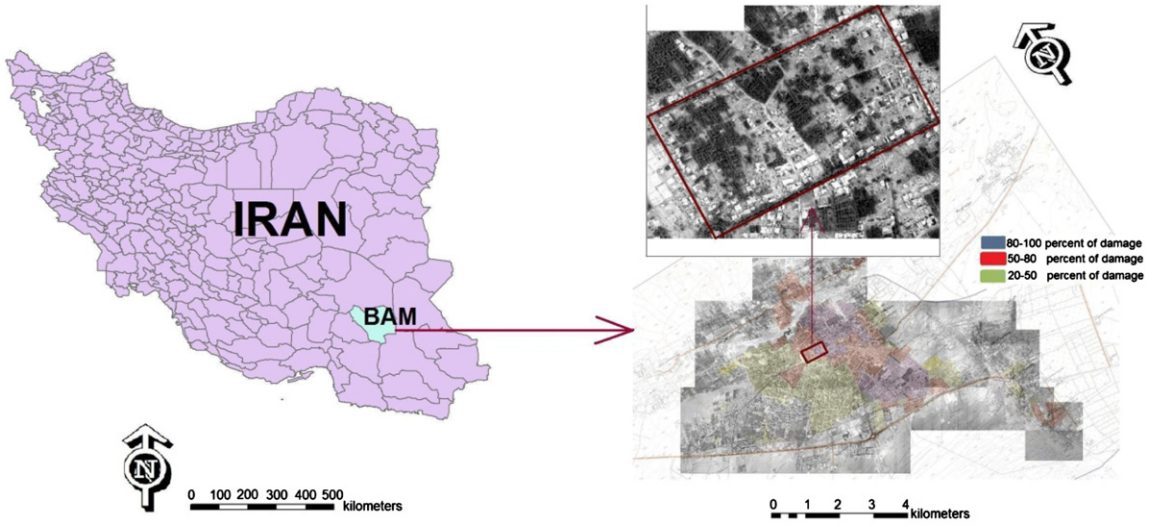

Fig. 8. City of Bam, the study area for validation of the proposed model: different damage levels caused by 2003 Bam earthquake (bottom right).

The sensitivity of the *MMI** in the study area ($d=32$ km) is calculated from Eq. (15) for small changes in d (i.e. an error of 0.1 in d results in an error of 0.006 in *MMI**).

$$\partial MMI^* = 0.06 \times \partial d \tag{15}$$

Small changes in the earthquake intensity result in changes in damage to buildings (Fig. 3). This effect is more sensible in the middle section of the fragility curves with a steep slope where a 0.1 shift in *MMI* results in about 6% change in the damages. For the earthquake scenario in this paper (with a 6.4 magnitude), small changes in *MMI* does not affect the damage to building type 9 (Table 2), because the curve's slope is zero in this magnitude range. The small changes in *MMI* affects the amount of damage to building types 5, 6, 7 and 8 more than building types 1, 2, 3 and 4 because the first group's fragility curves are steeper in this magnitude range. The above results are summarized in Table 5, which illustrates that the earthquake magnitude, the amplification in the velocity band and the distance to the earthquake source have the most effect on the model's output, respectively.

7. Summary and conclusions

The Iranian Plateau is marked by active faulting, active folding, fluctuating crustal thickness, mountainous terrain and recent volcanic activities and it has, consequently, experienced numerous catastrophic earthquakes. Tehran also hosts many industries, fuel and oil reservoirs and crucial infrastructure that serve local, regional and national interests. A major earthquake could cause disastrous damage near its epicenter and further harsh consequences for a much wider region. Any such crisis would be much more immense than the earthquake simulated by this paper.

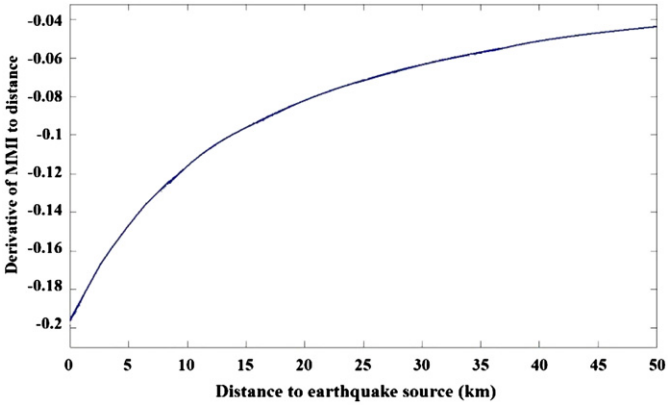

Fig. 10. The derivative of *MMI** to the distance to the earthquake source (d).

Earthquake loss assessments are predictions of damage and human and economic impacts from probable future earthquakes. They are not exact forecasts, but rather, they draw on recent scientific and engineering knowledge to estimate damage. Such damage estimation methods vary from district to district. This paper presents a methodology for evaluation of earthquake-induced damages to structures, people and streets in order to identify urban regions most likely to undergo significant human and structural losses during a major earthquake. The application of this method to a parish in Tehran proved to be an effective approach and the results of this study have great significance to loss mitigation during likely seismic events given that they identify opportunities to design and implement disaster management strategies. The estimated damages can help disaster-managers in two ways; first, to plan short-term strategies to reinforce less vulnerable buildings and long-term strategies to reconstruct more strong buildings and widen quite blocked streets. Second, to plan relief operation in advance, considering street blockages and fatalities.

The ground shaking effect and signature on buildings and other structures has been calculated via *MMI* attenuation relations. Earthquake scenario, earthquake source characteristics, site-specific geological, geotechnical data and local geology were considered in an intensity estimation.

Damage to each building was calculated based on specifically designed fragility curves. The casualties, street blockages and settlement accessibility were estimated and displayed using new GIS methods.

This paper highlights that earthquake damages and casualties would be great, despite considering a magnitude less than predicted for the Mosha Fault, further indicating a need to retrofit and renovate buildings and widen streets. Secondly, the analysis of massive spatial data used in this study proves the usefulness of GIS in this field.

The validation of the model using the Bam earthquake damages proved that the model overestimates the earthquake intensity. The resulted damages for the southern Karoon neighborhood in Tehran showed that about 63% of buildings will be totally destroyed. Also, considering the total blockage of about 22% of the streets by buildings waste materials, widening streets and preventing new adjacent buildings to exceed them are important precautions. Considering the similarity of the adjacent districts to the study area in land features, buildings type and streets, their state could almost be the same after the earthquake, even more catastrophic in southern Tehran because of denser population and more vulnerable structures. Therefore, the urban managers should accentuate the results of such native studies to prevent tragic irrecoverable events.

Table 5
The effect of small changes of different parameters on *MMI** and damages to buildings.

An error of 0.1 in the parameter	Explanations	Results in an error in *MMI**	Explanations	Results in an error in damage percent (%)
The earthquake magnitude (M)		0.140	For building types 1,2,3,4 and $M=6.4$	6
			For building types 5,6,7,8 and $M=6.4$	8
			For building type 9 and $M=6.4$	0
The amplification in the velocity band (F_v)	The F_v is assumed 1.4	0.108	For building types 1,2,3,4 and $M=6.4$	4
			For building types 5,6,7,8 and $M=6.4$	6
			For building type 9 and $M=6.4$	0
The distance to the earthquake source (d)	The d is assumed 32 km	0.006		0

The sensitivity analysis of model parameters showed that small changes in the earthquake magnitude, the amplification in the velocity band and the distance to the earthquake source have most effect on the model's output, respectively.

The proposed method is applicable anywhere in any earthquake-prone areas with the potential for future earthquakes. This study could be enhanced by first expanding the model to include other influential factors on losses such as secondary hazards. Additionally, the proposed model could be expanded to simulate different reactions to earthquake scenarios and provide relief and instructional programs.

Acknowledgment

We would like to express our gratitude to Dr. Mohamad Reza Zolfaghari at K.N. Toosi University of Technology, who shared his knowledge and experiences with us to improve the paper.

Appendix A. Supplementary Material

Supplementary data associated with this article can be found in the online version at doi:10.1016/j.soildyn.2011.07.003.

References

[1] Montoya L, Masser I. Management of natural hazard risk in Cartago, Costa Rica. Habitat International 2005;29:493–509.
[2] Branscomb LM. Sustainable cities: safety and security. Technology in Society 2006;28:225–34.
[3] Handmer J, Dovers S. Handbook of disaster and emergency policies and institutions. Earthscan Publications; 2007.
[4] Olsen GR, Carstensen N, Hoyen K. Humanitarian crisis: what determines the level of emergency assistance? Media coverage, donor interest and the aid business Disasters 2003;27:109–26.
[5] Karimi I, Hüllermeier E. Risk assessment system of natural hazards: a new approach based on fuzzy probability. Fuzzy Sets and Systems 2007;158:987–99.
[6] Drabek TE, Hoetmer GJ. Emergency Management: Principles and Practice for Local Government. Washington, DC: International City Management Association; 1991.
[7] Xu L, Liu G. The study of a method of regional environmental risk assessment. Journal of Environmental Management 2009;90:3290–6.
[8] Schneider PJ, Schauer BA. HAZUS—Its development and its future. Natural Hazards Review 2006;7:40–4.
[9] Vahidnia MH, Alesheikh AA, Alimohammadi A, Hosseinali FA. GIS-based neuro-fuzzy procedure for integrating knowledge and data in landslide susceptibility mapping. Computers & Geosciences 2010;36:1101–14.
[10] Westen CV. Geoinformation science and earth observation for municipal risk management; The SLARIM project. International Instititute for Geoinformation Science and Earth Observation, ITC; 2004.
[11] Federal Emergency Management Agency (FEMA). Multi-hazard loss estimation methodology: earthquake model (HAZUS-MHMR1), Technical manual; 2003.
[12] Michalowski W, Kersten G, Koperczak Z, Szpakowicz S. Disaster management with NEGOPLAN. Expert Systems With Applications 1991;2:107–20.
[13] Bird JF, Bommer JJ. Earthquake losses due to ground failure. Engineering Geology 2004;75:147–79.
[14] Ergonul S. A probabilistic approach for earthquake loss estimation. Structural Safety 2005;27:309–21.
[15] Feyza Cinicioglu S, Bozbey I, Oztoprak S, Kubilay Kelesoglu M. An integrated earthquake damage assessment methodology and its application for two districts in Istanbul, Turkey. Engineering Geology 2007;94:145–65.
[16] Srinivas H, Nakagawa Y. Environmental implications for disaster preparedness: lessons learnt from the Indian Ocean Tsunami. Journal of Environmental Management 2008;89:4–13.
[17] Tinguaro Rodriguez J, Vitoriano B, Montero J. A general methodology for data-based rule building and its application to natural disaster management. Computers and Operation Research, in press. doi:10.1016/j.cor.2009.11.014.
[18] Ansal A, Akinci A, Cultrera G, Erdik M, Pessina V, Tonuk G, et al. Loss estimation in Istanbul based on deterministic earthquake scenarios of the Marmara Sea region (Turkey). Soil Dynamics and Earthquake Engineering 2009;29:699–709.
[19] Ashtari M, Hatzfeld D, Kamalian N. Microseismicity in the region of Tehran. Tectonophysics 2005;395:193–208.
[20] Doloei J, Roberts R. Crust and uppermost mantle structure of Tehran region from analysis of teleseismic P-wave form receiver functions. Tectonophysics 2003;364:115–33.
[21] Martini PM, Hessami K, Pantosti D, D'Addezio G, Alinaghi H, Ghafory-Ashtiani M. A geologic contribution to the evaluation of the seismic potential of the Kahrizak fault (Tehran, Iran). Tectonophysics 1998;287:187–99.
[22] Ashtari Jafari M. Statistical prediction of the next great earthquake around Tehran, Iran. Journal of Geodynamics 2010;49:14–8.
[23] Sadidkhouy A, Javan-Doloei G, Siahkoohi HR. Seismic anisotropy in the crust and upper mantle of the Central Alborz Region, Iran. Tectonophysics 2008;456:194–205.
[24] Yaghmaei-Sabegh S, Lam NT. Ground motion modelling in Tehran based on the stochastic method. Soil Dynamics and Earthquake Engineering 2010;30:525–35.
[25] Abbassi A, Nasrabadi A, Tatar M, Yaminifard F, Abbassi MR, Hatzfeld D, et al. Crustal velocity structure in the southern edge of the Central Alborz (Iran). Journal of Geodynamics. 2010;49:68–78.
[26] Zafarani H, Noorzad A, Ansari A, Bargi K. Stochastic modeling of Iranian earthquakes and estimation of ground motion for future earthquakes in Greater Tehran. Soil Dynamics and Earthquake Engineering 2009;29:722–41.
[27] Hamzehloo H, Vaccari F, Panza GF. Towards a reliable seismic microzonation in Tehran, Iran. Engineering Geology. 2007;93:1–16.
[28] Japan International Cooperation Agency (JICA) & Center for Earthquake and Environmental Studies of Tehran (CEST) & Tehran Municipality. The study on seismic microzoning of the Greater Tehran area in the Islamic Republic of Iran. Final report; 2000.
[29] Kleindorfer PR, Sertel MR. Mitigation and Financing of Seismic Risks: Turkish and International Perspectives. Dordrecht, Netherlands: Springer; 2001.
[30] Chernov YK. Strong Ground Motion and Quantitative Estimation of Seismic Hazard. Tashkent: Fan Publishing House; 1989.
[31] Chernov YK, Sokolov VY. Correlation of seismic intensity with fourier acceleration spectra. Physics and Chemistry of Earth (A) 1999;24:523–8.
[32] Gupta IM. A note of correlation of Modified Mercalli Intensity with peaks of far-field ground motion. Bulletin of Seismological Society of America 1980;70:925–32.
[33] Murphy JR, O'Brien JL. The correlation of peak ground acceleration amplitude with seismic intensity and other physical parameters. Bulletin of Seismological Society of America 1977;67:877–915.
[34] Nazarov AG, Shebalin NV. Seismic Scale and the Methods of Seismic Intensity Measuring. Moscow: Nauka Publishing House; 1975.
[35] Ohta Y, Ohashi H, Ergunay O, Tabban A. Seismic intensity and its application to engineering: a study in Turkey. Strong Ground Motion Seismology 1987:385–401.
[36] Trifunac MD, Brady AG. On the correlation of seismic intensity scales with the peaks of recorded strong ground motion. Bulletin of Seismological Society of America 1975;65:139–62.
[37] Crespellani T, Vannuchi G, Zeng X. Seismic hazard analysis, Seismic hazard and site effects in the Florence Area. In: Proceedings of the Xth European conference on soil mechanics and foundation engineering 1991; p. 11–31.
[38] Borcherdt RD. Spatial ground motion amplification analysis. Proceedings of Geo-Logan 1997:56–69.
[39] Shafiee A, Azadi A. Shear-wave velocity characteristics of geological units throughout Tehran City, Iran. Journal of Asian Earth Sciences 2007;29:105–15.
[40] AS/NZS 1170.4. Draft Australian/New Zealand Standard for Structural Design Actions, Part 4: Earthquake Actions in Australia. Document No. D5212-5.1 issued in Standards Australia and Standards New Zealand; June 2005.
[41] Lam, N.T., Gaull, B.A., & Wilson, J.L. Calculation of earthquake actions on building structures in Australia. EJSE Special Issue: Loading on Structures; 2007.
[42] Askan A, Yucemen MS. Probabilistic methods for the estimation of potential seismic damage: application to reinforced concrete buildings in Turkey. Structural Safety 2010;32:262–71.
[43] Rossetto T, Elnashai A. Derivation of vulnerability functions for European-type RC structures based on observational data. Engineering Structures 2003;25:1241–63.
[44] Coburn A, Spence R. Earthquake Protection. second ed. West Sussex, England: Wiley; 2002.
[45] United States Geological Survey (USGS). Website: 〈http://www.usgs.gov〉.
[46] Ramazi H, Soltani Jigheh H. The Bam (Iran) Earthquake of December 26, 2003: from an engineering and seismological point of view. Journal of Asian Earth Sciences 2006;27:576–84.
[47] Ahmadizadeh M, Shakib H. On the December 26, 2003, southeastern Iran earthquake in Bam region. Engineering Structures 2004;26:1055–70.
[48] Building and Housing Research Center (BHRC). Iranian code of practice for seismic resistance design of buildings. Iranian Building Codes and Standards, Standard No. 2800. third ed.1999.